

## NUMERICAL SIMULATION OF CHOKED TWO-PHASE FLOW FOR HAZARDOUS AREA CLASSIFICATION

**Paloma L. Barros**  
**Claudemi A. Nascimento**  
**Ranny R. Freire**  
**Francisco J. de Queiroz**  
**Antônio T. P. Neto**  
**José J. N. Alves**

*paloma.lins@eq.ufcg.edu.br*

*claudemi.alves@eq.ufcg.edu.br*

*ranny.freire@eq.ufcg.edu.br*

*josimar.queiroz@eq.ufcg.edu.br*

*tavernard@eq.ufcg.edu.br*

*jailson@eq.ufcg.edu.br*

*Federal University of Campina Grande*

*882 Aprigio Veloso, 58429-900, Paraiba/Campina Grande, Brazil*

**Abstract.** Two-phase flashing jet is the type of flow that results from the release of liquefied gas into the atmosphere. The study of this multiphase release is of particular interest in industrial risk assessments, especially when hazardous area classification analysis is applicable. The understanding of those release phenomena using numerical techniques is relevant since it contributes with reliable data when experimental setup of several scenarios is not feasible. Both the behavior and the characteristics of these two-phase flow can significantly affect the hazard zone, it means that as more accurate the flashing jet model is, the more rigorous is the definition of the hazardous area. Hence, this work aims to propose a Computational Fluid Dynamic model to predict choked two-phase flow, thus a more reliable vapor cloud shape can be obtained. The Leung model was implemented for calculating critical conditions of a propane leak, along with a Eulerian-Lagrangian approach for particle tracking and Shear Stress Transport turbulence model in Ansys CFX<sup>®</sup> software. Simulation results show the plume extent and volume within a safety factor of the lower explosivity limit, velocity and molar fraction profiles along the jet axis, and shock wave prediction expressed through the Mach number profile. The present work demonstrates that the predicted spread angle outcome is crucial to determine the plume volume and, consequently, to quantify the risk factor.

**Keywords:** Choked flow, Hazardous area classification, CFD; Two-phase leakage

## 1 Introduction

Two-phase jets result from liquefied gases release into the atmosphere. The risk assessment in places where flammable substances are handled, mainly oil and gas industries, is one of the main concerns related to multiphase jets studies. In such scenarios, hazardous area classification methods must be applied in order to minimize the risk of explosions. The potential risk involved is characterized by the presence of an explosive atmosphere subject to the following factors: probability of flammable substance leakage, the nature of the emission, and ventilation availability [1].

An explosive atmosphere is formed when a vapor cloud, with sufficient concentration of flammable components, coexists with atmospheric air. This scenario enables flame propagation after ignition. Hence, in locations where there is a probability of formation of an explosive atmosphere – called a hazardous area – precautions need be taken aiming at minimize the likelihood of accidental ignition. Area classification method arise as a tool which defines criteria for hazardous areas assessment, as well as identification of different regions (zones) according to the probability of explosive atmospheres occurrence.

The extent of a hazardous zone is defined based on the flammable concentration in the atmosphere. However, after a leakage, can be assured that all possible flammable vapor/ambient air mixture compositions occur within the jet release location and the far field of the jet [2]. Therefore, the extent of the zone should be linked to the lower flammability limit (LFL). LFL means the lower concentration of a flammable substance/air mixture that can produce an explosive atmosphere

A classified area demands adequate management, starting from the construction to the installation and maintenance of electrical equipment. The use of area classification techniques seeks economically feasible projects with proper safety. Zohdirad *et al.* [3] emphasize that underestimating classified areas are considered as errors and should be avoided. On the other hand, overestimation can become quite costly. Thus, the accurate prediction of hazardous extent is one of the main challenges within area classification.

Explosion risk management is based on industrial, national and international standards, which usually establish conservative parameters to provide hazardous area classification analyses. Among them, the international standard IEC 60079-10-1 also recommends the use of auxiliary tools, and Computational Fluid Dynamics (CFD) is an important one. Confronted with this, numerical analyses emerge as an alternative to more accurate studies, avoiding conservative results. Souza *et al.* [4] and Alves *et al.* [5], for example, present numerical studies of gas leaks validated against experiments, which contribute to application of CFD models for hazardous area classification.

Understanding the behavior of flammable substances leaks by using CFD techniques is relevant to provide reliable data, especially when experimental scenarios may be unfeasible. However, although numerical simulation techniques improve the determination of essential parameters for area classification, literature consensus has not been reached regarding the prediction of two-phase emission conditions [6]. The uncertainties occur because of the complex characteristics presented in multiphase jets, such as the determination of physical properties under non-equilibrium thermodynamic conditions, and interactions between phases. The existing two-phase models for feed conditions calculations shall be carefully studied, analyzing the leaks both qualitatively and quantitatively, and expecting the prediction of known phenomena along the flow.

One of the possible scenarios of two-phase leakage is when the storage condition consists of a liquefied gas, which results in high momentum jets and shockwave formation. The Leung model [7] for critical flow is a valid approach in such situation, providing an analytical model for critical mass flow release prediction. Therefore, this work proposes to analyze two-phase jets of flammable substances via CFD, using the Leung model. This approach is then used to predict the hazardous area extent and the flammable volume that result from leaks in an un-obstructed open area.

## 2 Two-phase leakage

The two-phase release studies, within area classification context, demand development of models for liquid-vapor emission to predict the jet and the formation of gas plume. Epstein *et al.* [8] proposed a pattern of high momentum jet in which effects of buoyancy and atmospheric turbulence are negligible near the release point (as shown in Fig. 1). The flow is divided into three regions according to the emission behavior: 1) depressurization zone, where there are expansion and formation of aerosols; 2) jet entrainment, where the gas is diluted into atmospheric air; 3) plume dispersion at ground level.

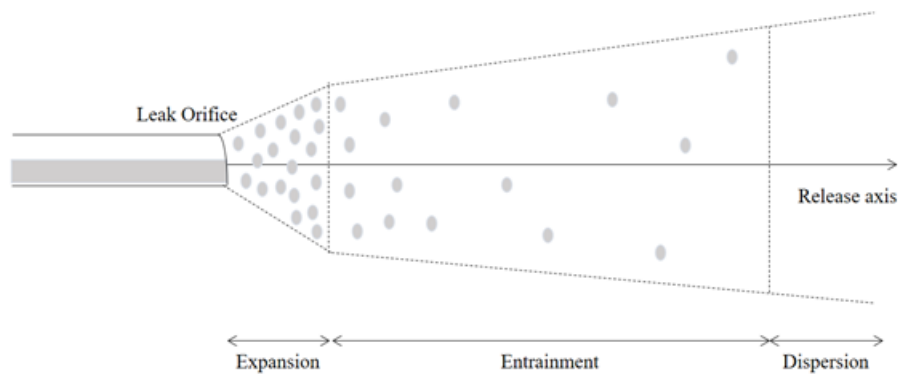


Figure 1. Two-phase flow release

Several authors have proposed and discussed models for multiphase leakages. Polanco *et al.* [9] present a review of theoretical, experimental and numerical approaches which evaluate liquid-vapor emissions. They emphasize that understanding the mechanisms involved in this type of release is important, mainly because it can prevent and minimize the impacts involved in accidental leaks. However, further studies can lead to more accurate two-phase jet prediction models in different scenarios. In that case, the nature of emissions is determined by a combination of variables: temperature, pressure, and orifice geometry are some of them. The correlation between those variables is not fully understood by the studies presented by Polanco *et al.* [9]

Calay and Holdo [10] propose a numerical approach via Computational Fluid Dynamics to study two-phase propane emission. The researchers evaluated different analytical expressions to determine the release rate, and the results were compared with experimental data obtained by Allen [11-12]. Considering the data analysis, it was suggested to calculate the two-phase jet release based on the liquid stagnation pressure, as well as to assume equal velocities for both phases. The model neglects the shock wave formation; thus, the computational domain encompasses the whole area apart from where this physical phenomenon takes place. In this case, the emission point setting is given by a computational diameter, also called as equivalent diameter.

Oliveira *et al.* [13] present CFD studies of horizontal multiphase jets in an open and unobstructed environment in order to apply the results for hazardous area classification. Their two-dimensional model consists of a Eulerian-Lagrangian approach, in which the inlet of the computational domain is defined after the expansion zone. That is, the results do not predict high momentum jet shock waves either. Not considering the expansion zone introduces some uncertainties in the calculations: an equivalent orifice diameter must be defined, as well as a release spreading angle value have to be predetermined by empirical equations.

In that scenario, CFD numerical analysis based on the critical conditions calculated by Leung model appears as an alternative treatment to reduce uncertainties due to shockwave disregard.

### 2.1 Leung model for critical flow

Leung [7] presents a general correlation for mass flux calculation in critical two-phase release,

depending entirely on stagnation conditions. This approach is based on the emission of a single component and considers a homogeneous model in thermodynamic equilibrium. The model introduces a correlation parameter  $\omega$  as follows.

$$\omega = \frac{x_o(v_{go} - v_{lo})}{v_o} + \frac{P_o}{v_o G_L^2} \quad (1)$$

Where  $x_o$  is the liquid fraction,  $v_{go}$  is the gas specific volume,  $v_{lo}$  is the liquid specific volume and  $P_o$  is pressure, all evaluated under storage conditions.  $G_L$  is the critical flow for the equilibrium-rate model for all-liquid inlet conditions, and depends on the following variables: vaporization enthalpy ( $\Delta H_o^{vap}$ ), liquid phase heat capacity ( $Cp_{lo}$ ) and storage temperature ( $T_o$ ).  $G_L$  is given by the following equation.

$$G_L = \frac{\Delta H_o^{vap}}{v_{go} - v_{lo}} \left( \frac{1}{Cp_{lo} T_o} \right) \quad (2)$$

If  $\omega \geq 4$ , the critical mass flux is calculated according Eq. (3):

$$G = \frac{[0.6055 + 0.1356(\ln\omega) - 0.0131(\ln\omega)^2] \cdot \sqrt{P_o/v_o}}{\omega^{0.5}} \quad (3)$$

In contrast, if  $\omega < 4$ , the critical mass flux equation suggested by Leung [7] that best fits experimental data is:

$$G = \frac{0.66 \cdot \sqrt{P_o/v_o}}{\omega^{0.39}} \quad (4)$$

### 3 Methodology

#### 3.1 Geometry and meshing

The geometry of the computational domain was constructed starting from the real release orifice, whose dimensions are given in Fig. 2. For certain flammable substances releases in un-obstructed open area, symmetry about the horizontal axis can be considered as an assumption. In this study, a 4-degree cylindrical slice of the actual domain was constructed from the given dimensions, considering the symmetry axis as shown in Fig. 2. Thus, the geometry comes close to a two-dimensional domain.

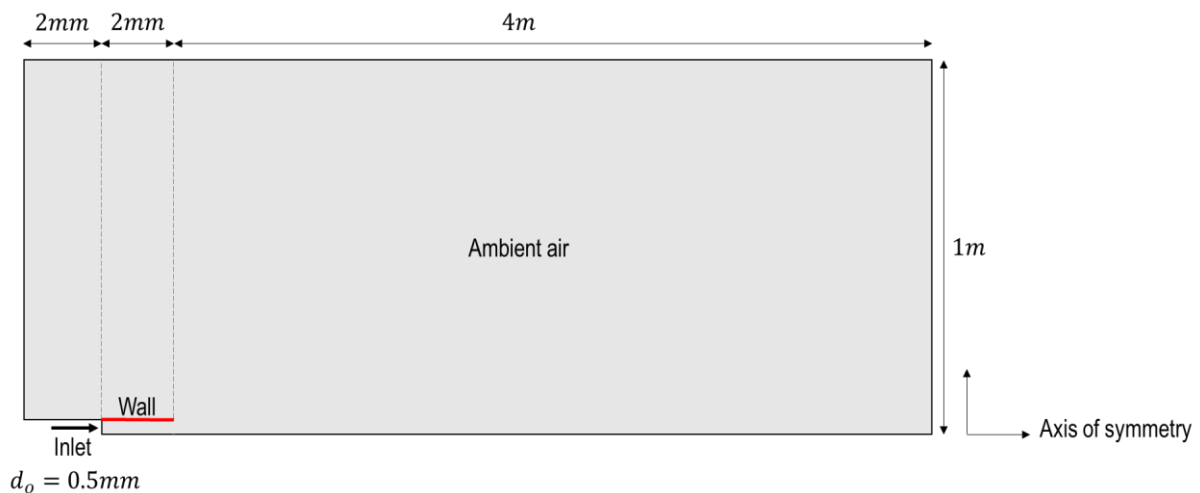


Figure 2. Dimensions of the computational domain

Secondly, a structured mesh with a high degree of refinement near the orifice was constructed, mainly to identify the shock wave phenomenon in this region (Fig. 3). A grid independence test was performed by varying the number of elements between 162,190 and 214,900. Table 1 shows values of the gas plume extent to LFL and to ½ LFL for each mesh under analysis.

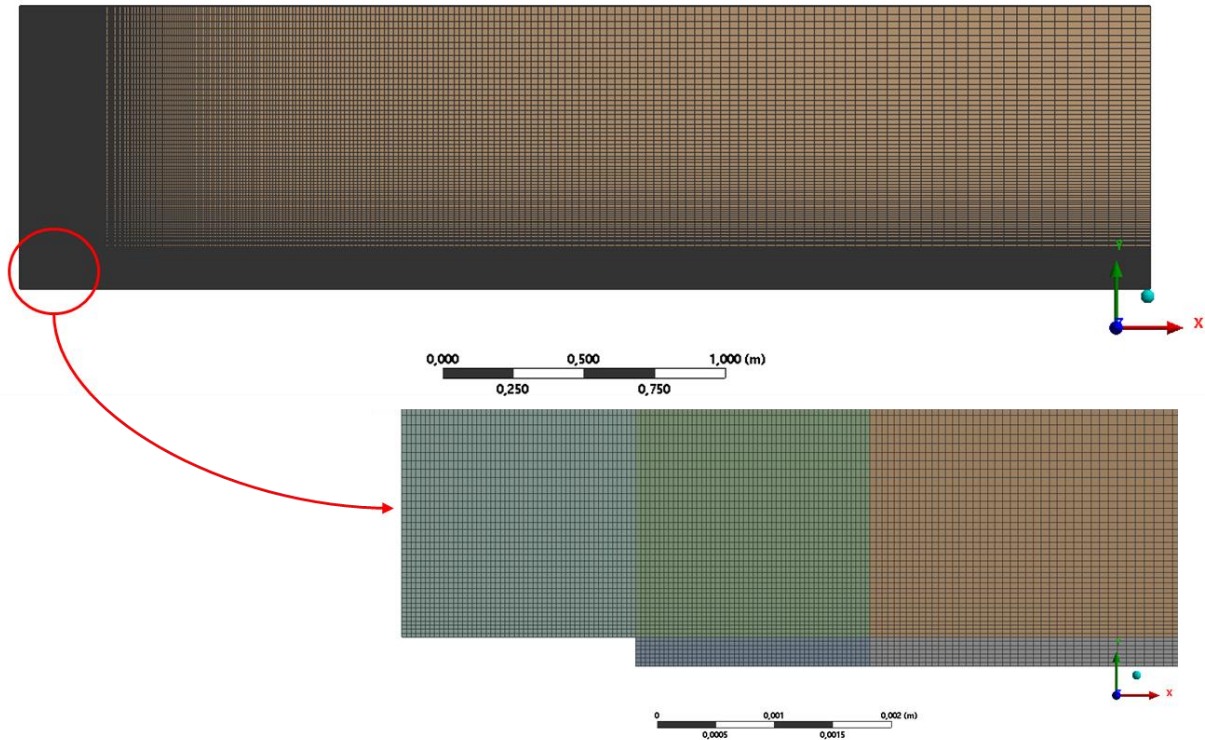


Figure 3. Computational mesh and detailed refinement

Table 1. Grid independence test

| Number of elements | Extent to LFL (m) | Extent to ½ LFL (m) |
|--------------------|-------------------|---------------------|
| 162,190            | 0.155721          | 0.306159            |
| 166,700            | 0.155725          | 0.306163            |
| 174,309            | 0.155734          | 0.306156            |
| 180,309            | 0.155734          | 0.306163            |
| 214,900            | 0.155765          | 0.306463            |

According to Table 1, it is possible to verify that the obtained results do not vary with computational mesh refinement. Therefore, the mesh containing 162,190 elements is already suitable for this work's simulation scenario.

### 3.2 Mathematical modeling

The multiphase model used a Eulerian-Lagrangean approach, in which the continuous phase is an atmospheric air/propane gas homogeneous mixture. Meanwhile, the particulate phase consists of liquid propane droplets. The steady state global continuity equations, species mass conservation, momentum, and energy for the continuous phase are presented as:

$$\nabla \cdot (\rho \vec{u}) = 0 \quad (5)$$

$$\nabla \cdot (\rho \vec{u} Y_i) = \nabla \cdot \left[ \left( \Gamma_{M_{eff}} \right) \nabla Y_i \right] + S_{MSi} \quad (6)$$

$$\nabla \cdot (\rho \vec{u} \times \vec{u}) = -\nabla p + \nabla \cdot \tau + S_M \quad (7)$$

$$\nabla \cdot (\rho \vec{u} H) = \nabla p + \nabla \cdot \left( \lambda \nabla T + \sum_{i=A,B,C}^{N_c} \frac{\lambda_i}{C p_i} h_i \nabla Y_i + \frac{\mu_t}{Pr_t} \cdot \nabla h \right) + S_E \quad (8)$$

Where  $\rho$  is the mixture density,  $\vec{u}$  is the velocity vector,  $Y_i$  is the mass fraction of component  $i$ ,  $\Gamma_{M_{i_{eff}}}$  is the effective molecular diffusion coefficient,  $S_{MSi}$  is the mass source,  $\tau$  is the tension tensor.  $S_M$  is the momentum source term,  $H$  is the specific enthalpy,  $p$  is pressure.  $\lambda$  is thermal conductivity,  $C p_i$  is heat capacity,  $h$  is enthalpy,  $\mu_t$  is turbulent viscosity,  $Pr_t$  is the Prandtl number, and  $S_E$  is the energy source term.

A one-way coupling between phases was defined. Thus, it means that the fluid movement does not affect the particle trajectory. Therefore, the particle drag force is no longer a momentum source for the continuous phase. Similarly, convective heat transfer, which occurs due to the temperature difference between the gas and the liquid surface, is neglected and it is not part of gas energy source terms.

The Shear Stress Transport (SST) turbulence model was adopted in this work as it provides high accurate results in case of a severe pressure gradient, and also covers transonic flow scenarios [14]. In addition, the particle tracking approach used Rosin-Rammler dispersion model for particle diameters. These droplets were injected in an equally spaced manner into the domain through the input orifice.

### 3.3 Boundary conditions

The critical mass flux was calculated using Eq. (4) for a propane leak stored as saturated liquid at 17 bar. A homogeneous equilibrium model was considered, that is, equal emission velocity for both phases, and physical properties calculated under equilibrium condition. The leakage orifice pressure is determined by Eq. (9) [13], whereas in thermodynamic equilibrium, the temperature at this point can be calculated by using Antoine equation.

$$P_e = 0.55 P_o \quad (9)$$

$$T_e = \frac{B}{A - \log_{10} P_e} - C \quad (10)$$

Where the parameters of Eq. (10) for propane are  $A = 7.01887$ ,  $B = 889.864$  and  $C = 257.084$ .

Moreover, the vapor mass fraction in the release orifice is calculated, and thereafter other physical properties of the mixture and boundary conditions can be obtained. Hence, Lees [15] presents Eq. (11) which defines the vaporized fraction of a superheated liquid in adiabatic condition as follows.

$$X_v = \frac{C p_l}{\Delta H_{vap}} (T_o - T_e) \quad (11)$$

Where  $C p_l$  is the heat capacity of the liquid phase, and  $\Delta H_{vap}$  is the enthalpy of vaporization. Then, the mixture density ( $\rho_m$ ) at the emission point can be calculated according to Eq. (12).

$$\rho_m = \frac{1}{X_v \frac{1}{\rho_g} + (1 - X_v) \frac{1}{\rho_l}} \quad (12)$$

By using both the mixture density and the critical mass flux, the two-phase critical emission velocity is calculated according to Eq. (13). Then, the mean particle diameter values immediately after the occurrence of the flashing [10] and the liquid mass flow were calculated by Eq. (14) and Eq. (15), respectively. The values obtained for propane properties and boundary conditions are presented in Tables 2 and 3.

$$V = \frac{G}{\rho_m} \quad (13)$$

$$d_{32} = 0.585 \frac{1}{V} \sqrt{\frac{\sigma}{\rho_l}} \quad (14)$$

$$m_l = GA_o(1 - X_v) \quad (15)$$

Where  $\rho_l$  is the liquid density,  $\sigma$  is the surface tension,  $m_l$  is the liquid mass flow rate, and  $A_o$  is the release orifice area.

Table 2. Physical properties of propane

| Properties  | Value      |
|---|------------|
| Heat capacity of liquid phase ( $J mol^{-1} K^{-1}$ ) | 127.6787   |
| Latent heat ( $J mol^{-1}$ )                          | 1.2792E+04 |
| Surface tension ( $N m^{-1}$ )                        | 0.0159     |
| Gas density ( $kg m^{-3}$ )                           | 16.7259    |
| Liquid density ( $kg m^{-3}$ )                        | 429.8708   |
| Density of the mixture ( $kg m^{-3}$ )                | 60.0183    |

Table 3. Boundary conditions

| Input data                       | Value       |
|----------------------------------|-------------|
| Inlet pressure ( $Pa$ )          | 9.3500E+05  |
| Inlet temperature ( $K$ )        | 296.5172    |
| Vapor fraction ( $wt\%$ )        | 0.2495      |
| Velocity ( $m s^{-1}$ )          | 126.3709    |
| Particle mean diameter ( $m$ )   | 28.1246E-06 |
| Liquid mass flow ( $kg s^{-1}$ ) | 0.0011      |

The computational domain includes opening conditions for far-field surfaces (ambient pressure and ambient temperature). The wall, as shown in Fig. 2, has a no slip condition for the gas phase. Also, the surfaces generated by the 4-degree revolution around the symmetry axis were set with symmetry condition.

For the Eulerian-Lagrangian approach, it was performed an independence test concerning the number of computational particles. That is, it was observed the effect of the number of simulated droplet trajectories along the flow. A range between 100 and 400 particles were simulated, and no significant changes regarding the primary expected results (extent of the hazardous area) were observed, as shown in Table 4. Therefore, the model with 100 computational particles was sufficiently adequate to represent the phenomenon.

Table 4. Effect of computational particles

| Number of particles | Extent to LFL (m) | Extent to $\frac{1}{2}$ LFL (m) |
|---------------------|-------------------|---------------------------------|
| 100                 | 0.155738          | 0.306166                        |
| 200                 | 0.155735          | 0.306161                        |
| 300                 | 0.155738          | 0.306157                        |
| 400                 | 0.155737          | 0.306158                        |

## 4 Results and discussion

Initially, it was verified the presence of the shock wave as a result of the simulation. The Mach number profile near the leakage region (Fig. 4) illustrates that the phenomenon was captured during the high momentum jet. In addition, Fig. 4 shows the spread angle formation following the expansion, which is a characteristic feature after the critical region.

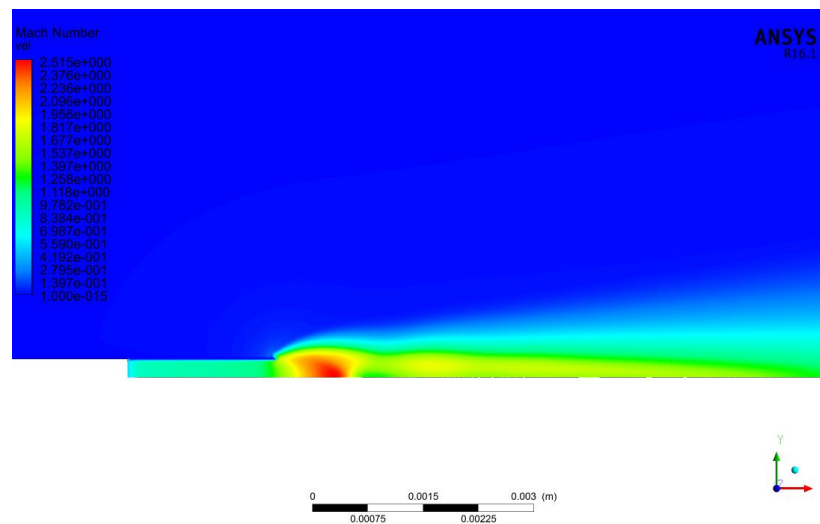


Figure 4. Mach number close to the orifice

Moreover, the particle temperature profile along the release axis can be analyzed in Fig. 5. It shows the rapid temperature decay of the liquid droplets, which is a result of the absorption of latent heat from the particles themselves for phase change. Verifying the temperature decrease is an important qualitative result, since this is a phenomenon described in the literature.

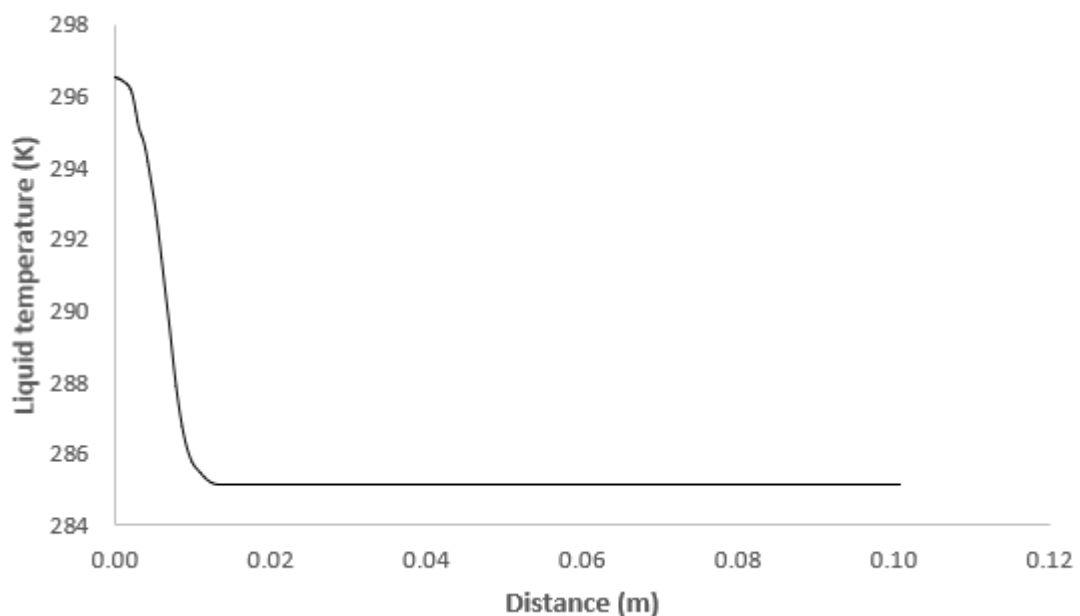


Figure 5. Liquid temperature profile



Regarding hazardous area classification, the most relevant outcomes are related to the gas concentration. This refers directly to the local potential danger, which depends on the lower flammability limits of the substance (2.1% vol for propane). Figure 6 illustrates the profile of propane gas molar fraction along the release axis; as expected, the concentration remains constant from the orifice to approximately 0.01m. After this, the mixture between propane and the atmospheric air becomes apparent until the complete dilution of the flammable gas into the atmosphere.

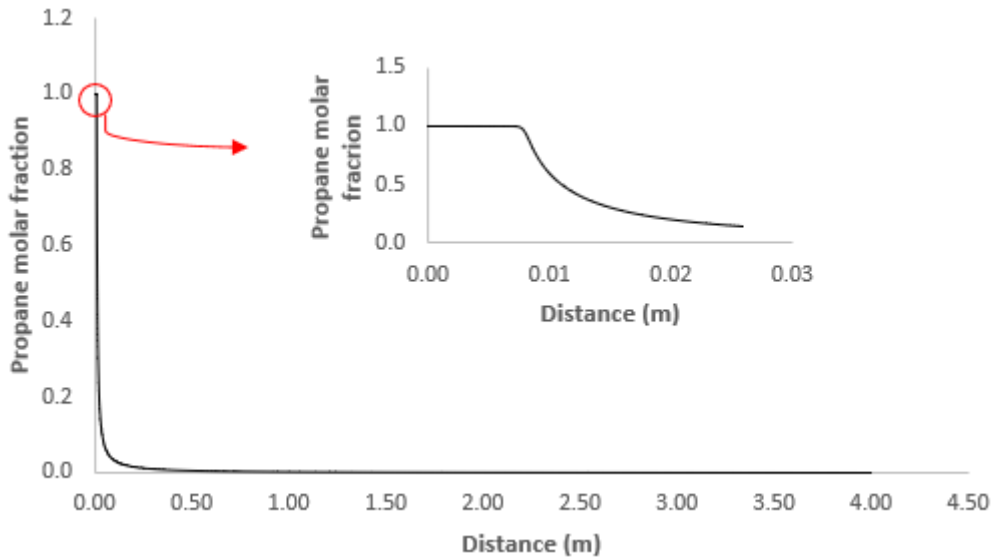


Figure 6. Propane molar fraction

Similarly, the propane molar fraction profile in the gas phase was evaluated over an axial plane, delimited by the LFL concentration. Figure 7 shows that the concentration of flammable gas decreases both radially and along the release axis.

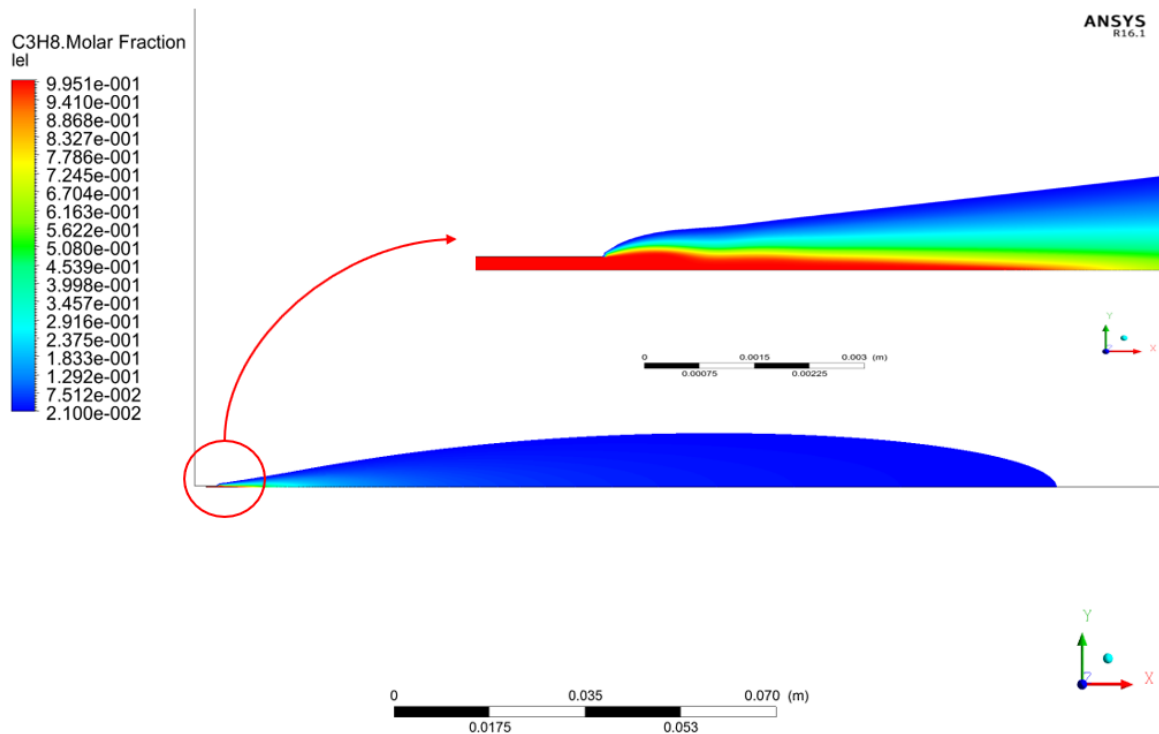


Figure 7. Surface profile of propane molar fraction

From the concentration profile, the extent and volume of the plume were defined, i.e. how far the hazardous zone should be delimited. This can be also obtained for ½ LFL in order to have a more conservative area classification result, within a safety factor of 100%. Table 5 shows the flammable extent and volumes obtained for both cases.

Table 5. Outcomes for hazardous area classification

| Extent to LFL<br>(m) | Extent to ½ LFL<br>(m) | Volume in LFL<br>(m <sup>3</sup> ) | Volume in ½<br>LFL (m <sup>3</sup> ) |
|----------------------|------------------------|------------------------------------|--------------------------------------|
| 0.156                | 0.306                  | 2.90E-05                           | 2.29E-04                             |

Finally, the risk factor can be estimated from Table 5. The calculation is given by the ratio of the plume volume in the LFL to the sphere volume (whose radius is the extent delimited by the LFL concentration).

$$R_f = \frac{V_{LFL}}{\frac{4}{3}\pi E_{LFL}^3} \times 100 \quad (16)$$

$$R_f = 0.183\%$$

The risk factor indicates the likelihood of meeting an explosive atmosphere in a hazardous area, considering that the emission of the flammable substance happened. For example, if the total volume of the classified area is filled with a flammable mixture with concentration above LFL, there is 100% probability of existing an explosive atmosphere there. This means that if an ignition occurs somewhere inside the zone extent, it will cause an accident. Hence, the two-phase release under the specific conditions described in this study results in a risk factor of 0.183%.

## 5 Final considerations

The numerical model implemented in this work described a two-phase jet of high momentum during an outdoor leakage of propane, using Leung's critical flow model. The simulation of this scenario allows the shock wave to be observed in the results, which increases the robustness for further application of the hazardous area classification method.

The hazardous area extent, to which safety measures must be taken to prevent possible ignition, is delimited according to the flammable plume size. In this case, an extent of 15.57cm at the lower flammability limit (LFL) and 30.62cm at ½ LFL was obtained. Moreover, the outcomes for the flammable volume were 2.90E-05m<sup>3</sup> and 2.29E-04m<sup>3</sup> at LFL and ½ LFL, respectively. The risk factor was also evaluated for the proposed scenario, presenting a 0.183% probability of meeting an explosive atmosphere around the release point in the classified area.

The CFD analysis of two-phase emission from critical conditions determined by Leung model has particular details, as the assumption of phase equilibrium. However, studying different models for leak condition calculations as well as using numerical tools enables a deeper analysis of the risks involved in liquid-vapor releases. As a consequence, the application of those studies in hazardous area classification technique can prevent conservative calculations while ensuring safe process conditions.

## Acknowledgements

The authors thank Capes por financial support for this study.

## References

- [1] A. McMillan. *Electrical installations in hazardous area*. Elsevier Science LTD, 1998.

- [2] M. Epstein and H. K. Fauske. Total flammable mass and volume within a vapor cloud produced by a continuous fuel-gas or volatile liquid-fuel release. *Journal of Hazardous Materials*, v. 147, pp. 1037-1050, 2007.
- [3] H. Zohdirad, T. Ebadi, S. Givehchi, and H. Meysami. Grid-based individual risk calculation in the classification of hazardous area with a risk-based approach. *Journal of Loss Prevention in the Process Industries*, v. 43, pp. 98-105, 2016.
- [4] A. O. Souza, A. M. Luiz, A. T. P. Neto, A. C. B. Araujo, H. B. Silva, K. S. Silva, and J. J. N. Alves. A new correlation for hazardous area classification based on experiments and CFD predictions. *Process Safety Progress*, v. 38, n. 1, pp. 21-26, 2018.
- [5] J. J. N. Alves, A. T. P. Neto, A. C. B. Araujo, H. B. Silva, S. K. Silva, C. A. Nascimento, and A. M. Luiz. Overview and experimental verification of models to classify hazardous areas. *Process Safety and Environmental Protection*, v. 122, pp. 102-117, 2019.
- [6] G. Giacchetta, M. Leporini, M. Marchetti, and A. Terenzi. Numerical study of choked two-phase flow of hydrocarbons fluids through orifices. *Journal of Loss Prevention in the Process Industries*, v. 27, pp. 13-20, 2014.
- [7] J. C. Leung. A generalized correlation for one-component homogeneous equilibrium flashing choked flow. *American Institute of Chemical Engineers*, v. 32, n. 10, pp. 1743-1746, 1986.
- [8] M. Epstein, H. K. Fauske, and G. M. Hauser. A model of the dilution of a forced two-phase chemical plume in a horizontal wind. *Journal of Loss Prevention in the Process Industries*, v. 3, pp. 280-290, 1990.
- [9] G. Polanco, A. E. Holdo, and G. Munday. General review of flashing jet studies. *Journal of Hazardous Materials*, v. 173, pp. 2-18, 2010.
- [10] R. K. Calay and A. E. Holdo. Modelling and dispersion of flashing jets using CFD. *Journal of Hazardous Materials*, v. 154, pp. 1198-1209, 2008.
- [11] J. T. Allen. Laser-based measurements in two-phase flashing propane jets. Part one: Velocity profiles. *Journal of Loss Prevention in the Process Industries*, v. 11, pp. 291-297, 1998a.
- [12] J. T. Allen. Laser-based measurements in two-phase flashing propane jets. Part two: Droplet size distribution. *Journal of Loss Prevention in the Process Industries*, v. 11, pp. 299-306, 1998b.
- [13] T. C. L. Oliveira, A. T. P. Neto, and J. J. N. Alves. CFD Simulation of flashing jet applied to area classification. *The Canadian Journal of Chemical Engineering*, v. 97, pp. 465-476, 2019.
- [14] F. R. Menter, 1993. Zonal two equation k- $\omega$  turbulence models for aerodynamic flows, *24<sup>th</sup> Fluid Dynamics Conference*, pp. 1-21.
- [15] F. Lees. *Lees' Loss Prevention in the Process Industries: Hazard Identification, Assessment and Control*. Butterworth-Heinemann, 3 ed. v. 1, 2005.